Observing and Modeling Earth's Energy Flows, Thirteen Years Later

Miklos Zagoni

Eotvos Lorand University, Faculty of Natural Sciences, Budapest, Hungary

e-mail: miklos.zagoni@t-online.hu

Abstract Observing and modeling energy flows in Earth's climate system was reviewed in an article in Surveys in Geophysics thirteen years ago as a concluding paper of a special collection with the same title. Analyzing their global mean energy budget estimate, a remarkable recognition can be made: there are specific small integer ratios among the flux components, as each of them are very close to an integer multiple of a unit flux, which is the longwave cloud radiative effect (LWCRE) with a value of 26.5 Wm^{-2}, as given in that study. Similar global energy budget estimates later by other authors, the IPCC and the NASA CERES science team show the same structure with convincing accuracy: typically, within the stated ranges of uncertainty. The physical science basis for the core flux components is identified in four radiative transfer constraint equations having their origin in the long-known two-stream approximation of Schwarzschild's equation; the fundamental integer ratios are solutions of the set of these four equations.

Keywords: global mean energy flow systems; integer relationships; radiative transfer equations

Introduction

A review article was published in Surveys in Geophysics thirteen years ago as a concluding study of a special collection with the same title (Stevens and Schwartz, 2012). Projecting longwave cloud radiative effect (LWCRE) on the energy flow distribution with the given CERES value of 26.5 Wm-2, it is easy to recognize that the flux components are integer multiples of that unit flux, close to the stated ranges of uncertainty; see Fig. 1.

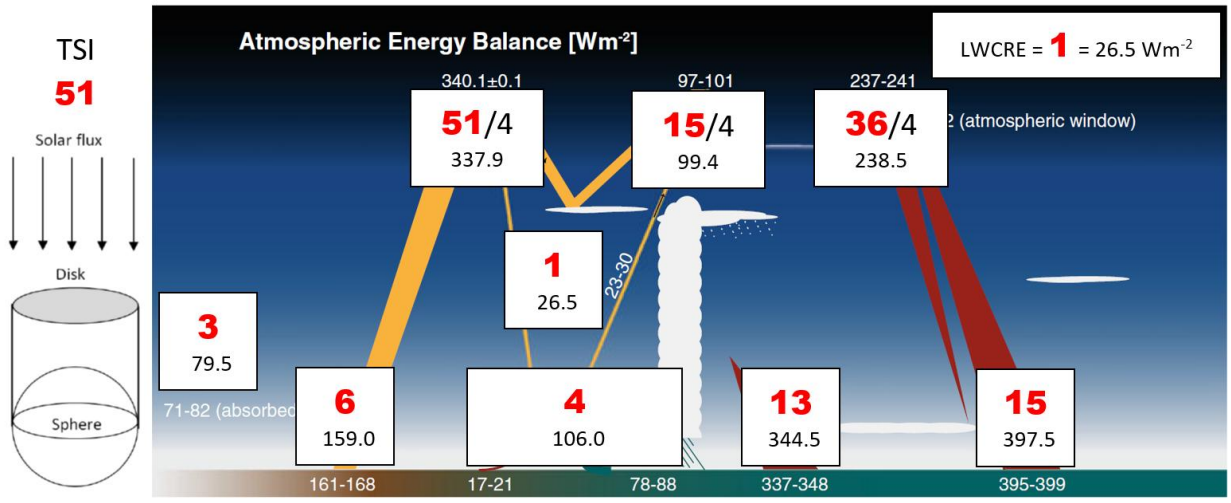

Fig. 1 Earth's global and annual mean energy flow system. Values are presented as a two-sigma range (Wm^{-2}). Original: Stevens and Schwartz (2012). We inserted LW CRE from their study, with their value from CERES EBAF. Numbers in red bold typeface are expressed in the unit of 26.5 Wm^{-2}. TOA fluxes are integers on the intercepting cross-section disk of incoming solar radiation.

At the top of the atmosphere (TOA), integer positions are quarters, that is, they are integers on the intercepting cross-section disk to incoming solar radiation, that is, before division by 4 for spherical weighting. Incoming solar radiation is smaller than the given lower limit by 2 Wm^{-2}. Atmospheric window is not part of the system. At the surface, integer position for absorbed solar radiation (6 units, with a value of 159.0 Wm^{-2}) falls out the indicated range of 161-168. Components of the convective flux (sensible heat and latent heat) do not fit separately into the integer system, but their sum (4 units = 106.0 Wm^{-2}) does. The position of total solar irradiance (TSI) is 51 units which, using the spherical factor, would be 1351.5 Wm^{-2}; with geodetic weighting (factor 4.0034, as in CERES EBAF), 1352.65 Wm^{-2}; still unacceptably low.

With these several exceptions, the appearance of the integer ratio system is interesting, but not convincing; without further indication, it may be regarded as a simple coincidence.

But later in that year, another update on global energy balance was published, based on the then-available best global observations (Stephens et al. 2012), where similar structures appear. First, the longwave cloud effect at TOA was upgraded to 26.7 (±4) Wm^{-2}, resulting in TSI = 51 units = 1361.7 Wm^{-2} (with the spherical multiplying factor of 4), or 1362.86 Wm^{-2} (with the geodetic formula of 4.0034). Since the then-accepted solar irradiance value was TSI = 1360.8 ± 0.5 Wm^{-2} (Kopp and Lean 2011), the latter would result in TSI/51 = 26.68 Wm^{-2} in the spherical case, and

26.66 Wm^{-2} in real-Earth geometry, supporting the fine-tuning in LWCRE. Integer positions for "Incoming solar" with the CERES geodetic factor of 4.0034 is 340.14 Wm^{-2}, and "Reflected solar" is 100.04 Wm^{-2} (340.2 and 100.0 are shown in the diagram).

Now with the value of 26.7 Wm^{-2}, given as the difference of "Clear-sky emission" (266.4) and "Outgoing longwave radiation" (all-sky emission, 239.7) in Fig. B1 of Stephens et al. (2012), these values themselves are integer multiples of this unit flux as 266.4 = 10 × 26.7 (and consequently 239.7 = 9 × 26.7) with a difference 0.6 Wm^{-2} only, which is far within the stated range of uncertainty (3.3), and equivalent to the indicated TOA imbalance. Similarly, at the surface, "Clear-sky emission to surface" (319) and "All-sky emission to surface" (345.6) differ by the longwave cloud effect at the surface (LWCRE SFC, 26.6), and these values are integer multiples of LWCRE SFC, as 319 = 12 × 26.6 with a difference of 0.2 Wm^{-2}, hence 345.6 = 13 × 26.6 (– 0.2 Wm^{-2}), compared to the stated ±9 Wm^{-2} uncertainty. Finally, "Surface emission" (398) also occupies an integer position, as 398 = 15 × 26.6, the difference is 1 Wm^{-2}, while the indicated uncertainty range is ±5 Wm^{-2}; the longwave part is shown in Fig. 2.

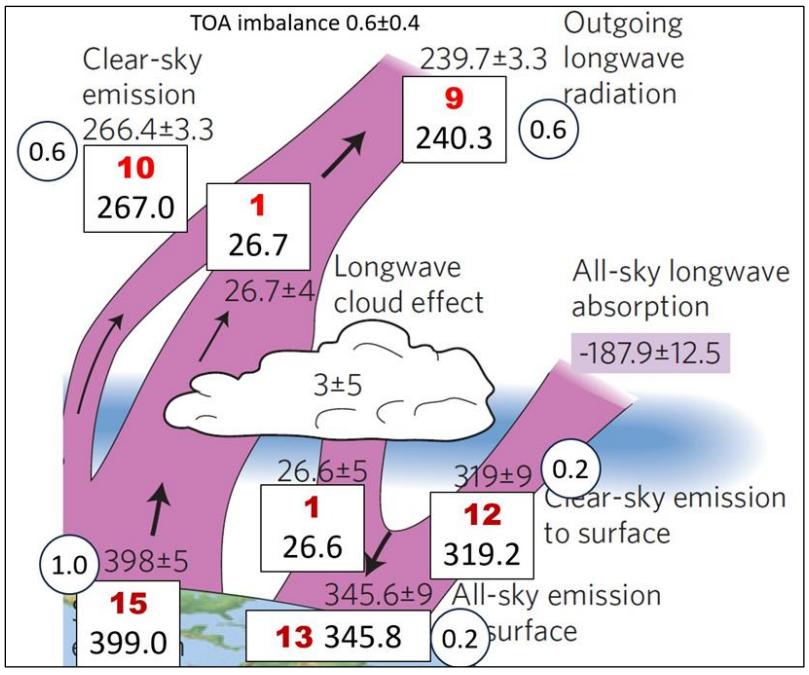

Figure 2 The longwave part of the global annual mean energy budget of Earth (Stephens et al. 2012, Fig.B1), with the integer system projected on it in textboxes. Red, bold typeface gives the integer values in units of one LWCRE at TOA (26.7 Wm^{-2}); purple values in units of one LWCRE at the surface (26.6 Wm^{-2}); the differences of the original values and the integer multiples are given in circles in Wm^{-2}.

Regarding the given uncertainty for LWCRE TOA as ± 4 Wm^{-2}, from now we will use one common unit flux for TOA and the surface.

Next year, another global mean energy budget distribution was presented (Wild et al. 2013), where the shortwave components were further updated, resulting in accurate positions in the integer system when using the same LWCRE TOA of 26.7 Wm^{-2} for unit flux as above. At TOA, incoming solar 340 occupies position of 51/4 (=340.4), where the division factor of four comes from spherical weighting; hence total solar irradiance TSI = 51 units = 1361.7 Wm^{-2}. Solar reflected (100) equals 15/4 = 100.1 with a difference of 0.1 Wm^{-2} only, resulting in an integer ratio for TOA albedo as 15/51, being arithmetically identical to the indicated 100/340. Absorbed solar and outgoing thermal radiation in equilibrium are equal with 9 units = 9 × 26.7 = 240.3 Wm^{-2}. Solar absorbed in the atmosphere is indicated as 79 Wm^{-2}; an integer position is 3 units = 80.1 Wm^{-2}, allowing solar down to the surface 185 Wm^{-2} in the diagram and 186.9 Wm^{-2} in the integer system as 7 units; with 161 Wm^{-2} solar absorbed at the surface in the diagram and 160.2 Wm^{-2} as 6 units in the integer system. The largest difference is in "Thermal down surface", given as 342 Wm^{-2}, when 13 units = 347.1 Wm^{-2}, so the bias is 5.1 Wm^{-2}, still within the noted uncertainty; see Fig. 3.

Even this discrepancy disappeared next year, when Loeb (2014) published a global mean energy budget based on CERES EBAF data. Refining the unit flux from 26.7 Wm^{-2} to 26.67 Wm^{-2}, the flux component "thermal down surface" (called here "Absorbed at Surface") in the integer ratio system is 346.7 Wm^{-2}; with a bias of 1.7 Wm^{-2} to the given value of 345 Wm^{-2} (this essential flux component, called also "Back radiation" was regarded as "another measure of the greenhouse effect" by Inamdar and Ramanathan 1997). The most peculiar feature here is that at the TOA, all three flux components (Incoming Solar, Reflected Solar and Outgoing LW Radiation) fit to their integer position with zero difference; see Fig. 4.

Next year again, NASA Energy and Water-cycle Study (NEWS) resulted in a global assessment of the joint cycles of energy and water (L'Ecuyer et al. 2015, Stephens and L'Ecuyer 2015). The important improvement here was new, upgraded values proposed to the components of convective flux separately: sensible heat (SH) = 25 Wm^{-2} and 26 Wm^{-2}, respectively, and latent heat (evaporation) = 81 Wm^{-2} and 82 Wm^{-2}, resp., close to integer positions of 1 unit = 26.67 Wm^{-2} and 3 units = 80.01 Wm^{-2}. Other flux components in the second-optimized version display well the integer system, see Fig. 5.

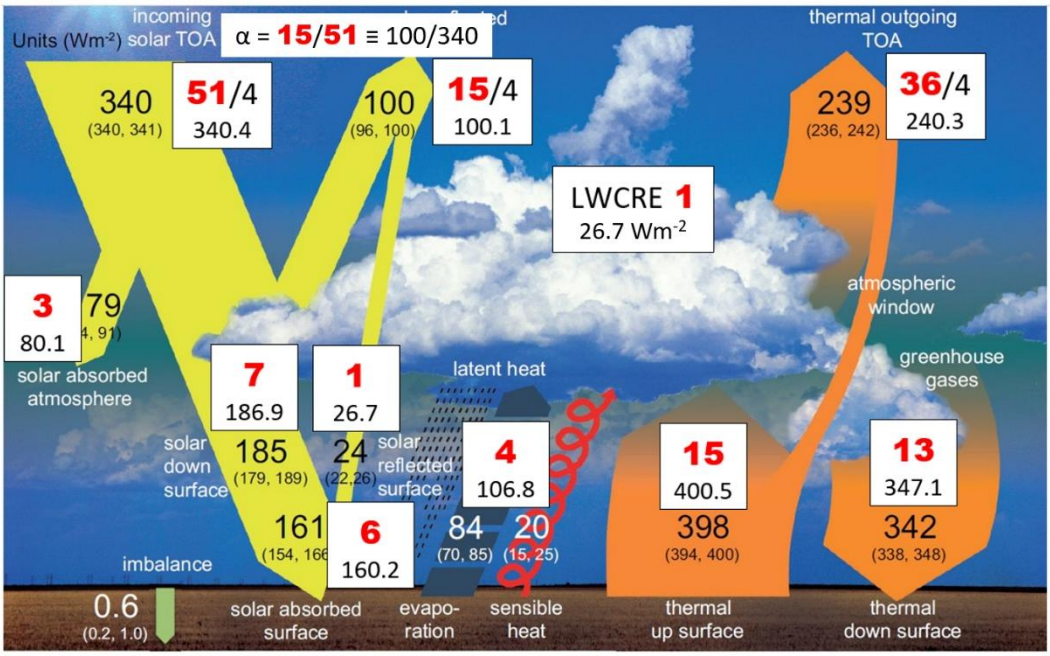

1

2 **Figure 3** Integer structure projected a global energy balance from a surface perspective (Wild et al. 2013,
3 appeared also in IPCC WGI AR5), using the same unit flux of 26.7 Wm^{-2} as above.

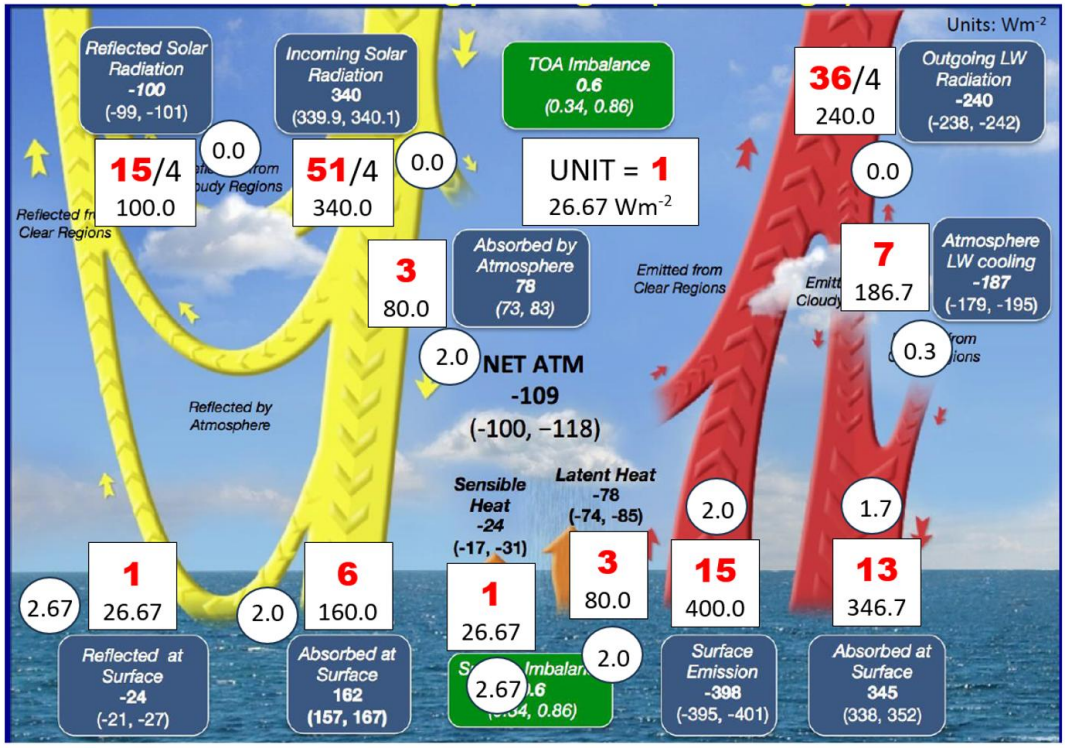

4

5 **Figure 4** Integer structure projected a global mean energy budget from CERES EBAF data (Loeb 2014)

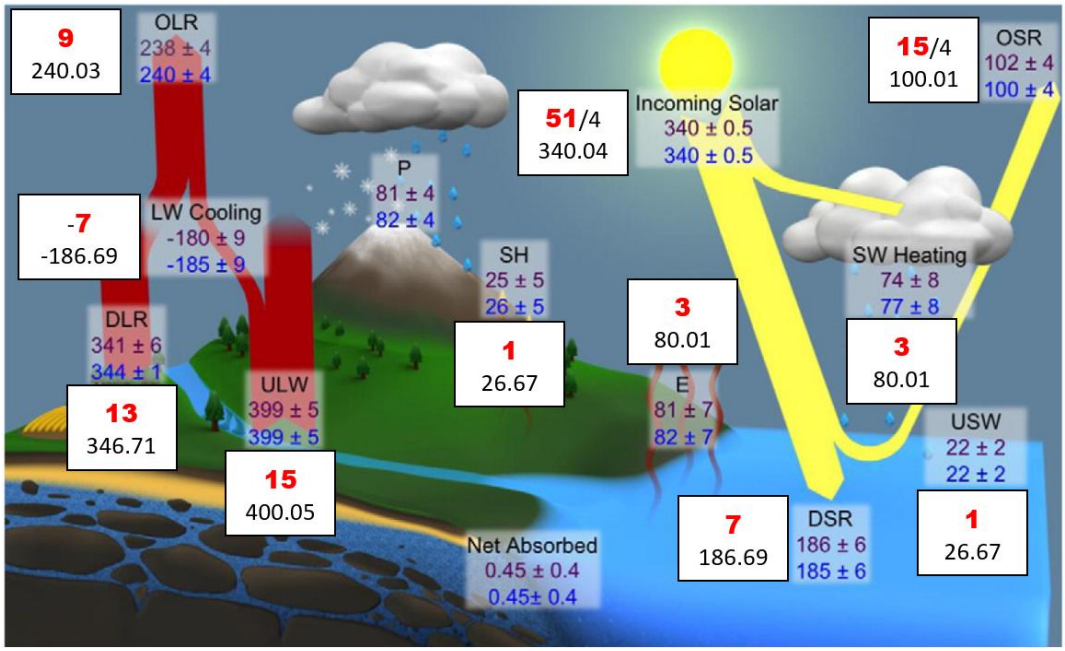

Figure 5 Global and annual mean Earth's energy balance (Stephens and L'Ecuyer 2015), with integer positions projected on it

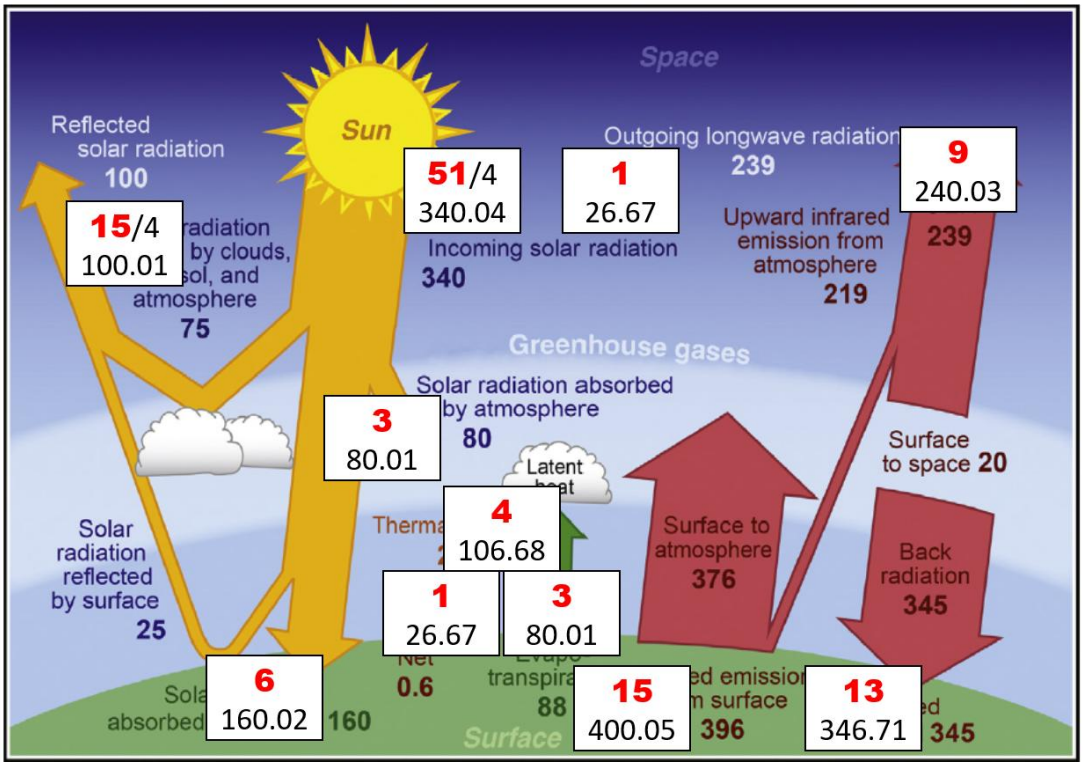

Figure 6 Global and annual average radiative and non-radiative energy-flow diagram for Earth and its atmosphere (Hartmann 2016, Fig. 2.4), with the integer system projected on it.

The increased value of 345 Wm^{-2} was accepted for the "Back radiation" in the second edition of Hartmann (2016). Using the same unit flux of 26.67 Wm^{-2} as above, the solar components of the energy flow system fit into the integer system within a robust accuracy of 0.04 Wm^{-2}; the largest difference is in the infrared emission from the surface, which was decreased from the IPCC and CERES EBAF value by 2 Wm^{-2}, to 396 Wm^{-2}. The components of the convective flux do not occupy integer positions separately; see Figure 6.

In the past decade, this higher value for the downward longwave radiation became widely accepted. In a current assessment of the global radiation budget from a surface perspective (Li, Li, Wild and Jones, 2024) based on 34 CMIP6 models, SW down radiation to the surface is 186±6, Reflect by surface = 24±3, convective flux (sensible heat + latent heat) = 106, Thermal down surface = 346±6, and Thermal up surface = 402±5 [Wm^{-2}]. The corresponding integer positions, with the same unit flux of 26.67 Wm^{-2} are as follows: 7 units = 186.69, 1 unit = 26.67, 4 units = 106.68, 13 units = 346.71, and 15 units = 400.05 [Wm^{-2}]; the differences are 0.69; 2.67; 0.68; 0.71, and 1.95 [Wm^{-2}], respectively — each of them far within the indicated uncertainty range.

At the top of the atmosphere, Stackhouse et al. (2024) provide a radiation budget from CERES satellite observations for 2001-2022. As shown in Table 1, with an upgraded unit flux of 26.68 Wm^{-2}, the difference of their climatological mean from the integer positions falls within, or close to (in the case of ASR), the interannual variability for the same period. Data taken from their Table 2.9.

Table 1 Global mean TOA radiative fluxes (Climatological Mean and Interannual Variability) from CERES, compared to the integer positions

Global	N	N × unit unit = 26.68 Wm^{-2}	Climatological Mean 2001-22 Wm^{-2}	Difference Wm^{-2}	Interannual Variability 2001-22, Wm^{-2}
OLR	36/4	240.12	240.35	0.23	±0.65
TSI	51/4	340.17	340.20	0.03	±0.15
RSW	15/4	100.05	99.00	1.05	±1.05
ASR	36/4	240.12	241.20	1.08	±1.05
Net	0	0	0.85	0.85	±0.85

The accuracy altogether is much better than expected from a simple coincidence, therefore an intense quest for a possible physical science basis was initiated. Four radiative transfer equations were identified and verified on published global energy flow distributions of CERES and GEWEX data, from which the integer ratios for the principal components arise as a solution.

Results

We utilize Schwarzschild's (1906, Eq. 11) two-stream radiative equilibrium model, consisting of three relationships (reproduced here in facsimile from the original; *E* emission of the surface; *A* upward beam, *B* downward beam given as the function of A_0, the emerging flux at the top-of-atmosphere, and *m*, the „optische Masse", optical depth):

$$(11) \qquad E = \frac{A_0}{2}(1+m), \quad A = \frac{A_0}{2}(2+m), \quad B = \frac{A_0}{2}m.$$

Our first equation will be the difference of the second and first terms:

$$\text{Eq. (1)} \qquad A - E = \Delta A = A_0/2,$$

yielding the net radiation at the surface, independently of the optical depth. It is reproduced and graphically represented in standard university textbooks like Goody (1964, Eq. 2.115); Houghton (1977, 1986, 2002, Eq. 2.13, Fig. 2.4); Chamberlain (1978, 1987, Eq. 1.2.29, Fig.1.4); Goody and Yung (1989, Eq.2.146); Hartmann (1994, 2016, Eqs. 3.48-3.54); Salby (1996, 2012, Eq. 8.67, Fig. 8.20); Pierrehumbert (2008, Eq. 4.45); Ambaum (2021, Eq. 10.56), and in university lecture notes (Stephens 2003, Eqs. 6.10a-b, Fig. 6.3a: $\pi T_S^4 - \pi T(\tau_S)^4 = \pi B_S - \pi B_0 = F\infty/2$), see Fig.7.

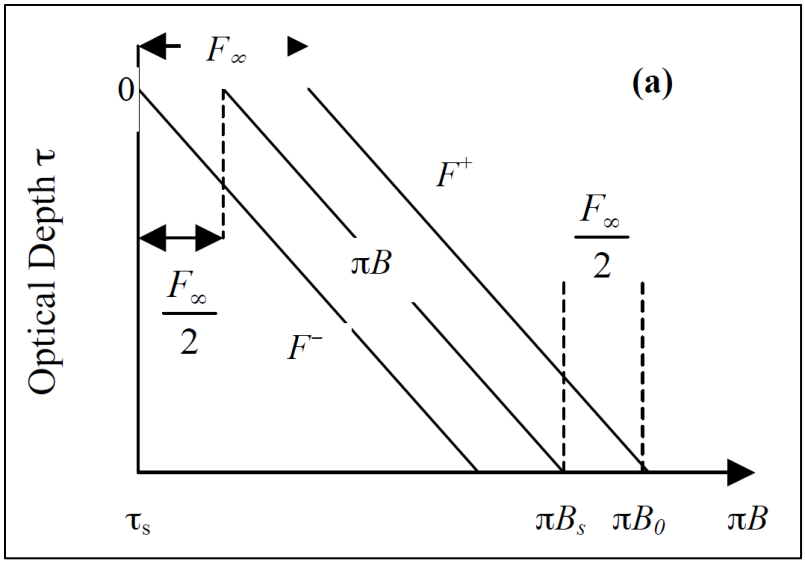

Figure 7 The flux profiles and blackbody function predicted by the simple gray body model as a function of optical depth (Stephens 2003, Fig. 6.3a)

Emden (1913) realized soon that in radiative equilibrium, Eq. (1) represents a temperature discontinuity at the surface, but in the same sentence he added that this jump ('*Temperaturspung*') "is greatly diminished by conduction of heat and evaporation". Authors generally note that "such a steep lapse rate is very unstable with respect to vertical motion, and will soon be destroyed by the process of convection" (Houghton 1977); "such discontinuities are usually are greatly suppressed in reality because of efficient heat transport by conduction and convection" (Hartmann 1994); "The solutions in Eqns. (6.10a) and (6.10b) predict a discontinuity between the surface temperature T_s and the air temperature just above the ground $T(\tau_S)$", and adds: "This radiative equilibrium profile is unstable w.r.t. vertical motion and is destroyed by convection" (Stephens 2003); "This temperature discontinuity is unstable in practice and there will be turbulent heat exchange which will remove the temperature discontinuity" (Ambaum 2021).

The equation states that the net radiation at the surface (R_N) in radiative equilibrium — and the corresponding convection in radiative-convective equilibrium — equals half of the outgoing longwave radiation (OLR) in the clear-sky:

Eq. (1) R_N (clear-sky) = SFC (SW net + LW net) (clear-sky) =
(SW down – SW up) + (LW down – LW up) (clear-sky) = OLR (clear-sky)/2.

As an initial justification, the equation was controlled on the then-available NASA CERES dataset, Energy Balanced and Filled (EBAF-Surface) Edition 2.8, data were taken from the Data Quality Summary (2015), Table 4.1:

Eq. (1) R_N (clear-sky) = SW down – SW up + LW down – LW up (clear-sky) = OLR(clear-sky)/2.

$$243.9 – 29.7 + 316.0 – 398.0 = 265.7/2 – 0.65$$

The equation is valid on that data product with a difference of 0.65 Wm^{-2}. [Note that Earth's heat uptake in that time was estimated as 0.58 ± 0.38 Wm^{-2} (Loeb et al. 2012).]

Since the first equation prescribes the convective flux (the sum of the sensible heat flux and latent heat flux) in a direct relationship to the outgoing longwave radiation (OLR) at TOA in the clear-sky, and convection changes almost linearly with sea surface temperature, a definite OLR-dependent convection assumes a definite, OLR-dependent surface upward longwave (ULW) thermal emission. Exploring possible formulas, as the optical depth (τ) of zero defines TOA, and $\tau = 1$ the level where OLR is initiated, Schwarzschild's formula for the surface (the middle term in Eq. 11) was tried at $\tau = 2$. Then the second equation gives the total SW + LW absorbed radiation (R_T) at the surface in the clear-sky:

Eq. (2) R_T (clear-sky) = (SW down – SW up + LW down) (clear-sky) = 2OLR(clear-sky).

CERES EBAF-Surface Ed2.8 Data Quality Summary (DQS) data [17]:

$243.9 – 29.7 + 316.0 = 2 \times 265.7 – 1.2$ Wm^{-2}.

This accuracy (compared to the estimated uncertainties in the EBAF-Surface data of 1σ between 3 and 7 Wm^{-2}, see Table 4.2 of [17]) was convincing enough to proceed further in this direction.

For all-sky, a third and fourth equations were created from the first pair, by separating atmospheric radiation transfer from the longwave effect of clouds (LWCRE) and using all-sky data on both sides:

Eq. (3) R_N (all-sky) = Surface SW net + LW net (all-sky) = [OLR(all-sky) – LWCRE]/2;

and

Eq. (4) R_T (all-sky) = Surface (SW + LW) absorbed (all-sky) = (SW down – SW up + LW down) (all-sky) = 2OLR (all-sky) + LWCRE.

Their accuracy on that data product was 2.65 Wm^{-2} for Eq. (3) and 2.10 Wm^{-2} for Eq. (4).

Controlling the four equations on EBAF Ed4.1_V3 data product, we have the biases of the individual equations within the range of ± 2.83 Wm^{-2}; and the mean bias of the four equations is 0.0007 Wm^{-2} (this justifies the use of four decimal places in the netCDF file), see Table 2. EBAF Edition 4.2 is also checked; with Version 4 data, first on the same period (April 2000-March 2022); the differences become as follows: -2.35, -2.70, 3.98, 3.46; the mean bias is 0.60 [Wm^{-2}]; then on the extended time period April2000-March 2024, and have -2.32, -2.50, 4.01, 3.67, with a mean of 0.715 [Wm^{-2}], still far within the absolute calibration uncertainty of the CERES instrument, and in the magnitude of the estimated Earth's Energy Imbalance.

Table 2 Verification of the four equations on CERES EBAF data

CERES EBAF Edition 4.1 Version 3, 22 years (April 2000 – March 2022) (Wm^{-2})
CERES EBAF Edition 4.2 Version 4, 22 years (April 2000 – March 2022) (Wm^{-2})
CERES EBAF Edition 4.2 Version 4, 24 years (April 2000 – March 2024) (Wm^{-2})

Eq. (1) R_N clear	**SFC SW dn**	**–SW up**	**+ LW down**	**–LW up**	**TOA LW/2**	**Diff**
Ed4.1, 22-yr	240.8680	–29.0724	+317.4049	–398.5211	266.0122 /2	–2.3267
Ed4.2, 22-yr	241.0969	–29.7521	+317.8744	–398.5890	265.9594 /2	–2.3495
Ed4.2, 24-yr	241.0514	–29.7043	+318.0984	–398.7742	265.9748 /2	–2.3161
Eq. (2) R_T clear	**SFC SW dn**	**– SW up**	**+ LW down**		**2 × TOA LW**	**Diff**
Ed4.1, 22-yr	240.8680	–29.0724	+ 317.4049		2 × 266.0122	–2.8238
Ed4.2, 22-yr	241.0969	–29.7521	+ 317.8744		2 × 265.9594	–2.6996
Ed4.2, 24-yr	241.0514	–29.7043	+ 318.0984		2 × 265.9748	–2.5042
Eq. (3) R_N all	**SFC SW dn**	**– SW up**	**+ LW down**	**– LW up**	**(TOA LW – LWCRE)/2**	**Diff**
Ed4.1, 22-yr	186.8544	–23.1629	+345.0108	–398.7550		+2.7083
Ed4.2, 22-yr	187.1451	–23.4950	+346.1057	–398.4220		+3.9818
Ed4.2, 24-yr	187.1756	–23.4607	+346.3158	–398.6162		+4.0126
Eq. (4) R_T all	**SFC SW dn**	**– SW up**	**+ LW down**		**2 × TOA LW + LWCRE**	**Diff**
Ed4.1, 22-yr	186.8544	– 23.1629	+ 345.0108		2 × 240.2450 + 25.7672	+2.4450
Ed4.2, 22-yr	187.1451	– 23.4950	+ 346.1057		2 × 240.3317 + 25.6277	+3.4647
Ed4.2, 24-yr	187.1756	– 23.4607	+ 346.3158		2 × 240.3894 + 25.5854	+3.6665
					Mean	0.0007
						0.5994
						0.7147

This unprecedented accuracy of the constraint equations raises a couple of questions. Do these four equations express an arithmetic identity? The answer is no; in the prevailing theory we are not aware of any relationship that would require these couplings between surface and TOA irradiances, without referring to any atmospheric gaseous composition or the optical depth. Or, are these four equations built in the CERES data production protocol? No again: the mean bias in the first five years vary between -0.5 and -0.2 [Wm^{-2}] and it approaches zero after including 17 years into the averaging; then it occupies the value of zero and remains there after only two decades.

Notice that the clear-sky equations prescribe the ratio

R_N : (TOA_LW_up) : (SFC_LW_up) : R_T = 1 : 2 : 3 : 4 ,

resulting in a clear-sky greenhouse factor of

g(clear-sky) = G(clear-sky) / (SFC_LW_up) = [(SFC_LW_up) –(TOA_LW_up)] / (SFC_LW_up) = 1/3.

With CERES EBAF Edition 4.2 V4 (24-yr) data (Table 1), g(clear-sky, CERES) = (398.7742 – 265.9748) / 398.7742 = 0.3330.

Recently, data were published from global energy and water cycle assessments on 30 years of the GEWEX mission (Stephens et al. 2023). Their data are for all-sky, therefore only equations (3) and (4) maybe controlled, with LWCRE taken from an earlier study of the same authors (Stephens et al. 2012) as 26.7 Wm^{-2}. According to Fig. 2 of the GEWEX study, net radiation at the surface (R) equals the sum of the convective fluxes: latent heat (evaporation) and sensible heat. Using data from Fig. SB3,

Eq. (3) R_N = LE + H = "Evaporation" + "Sensible heat" = (“Outgoing LW” –LWCRE)/2

81.1 + 25.4 = (239.5 – 26.7)/2 + 0.1 [Wm^{-2}]

Eq. (4) R_T = “Surface SW” – “Surface Reflection” + “All-sky emission” = 2 × “Outgoing LW” + LWCRE

184.0 – 23.3 + 345.1 = 2 × 239.5 + 26.7 + 0.1 [Wm^{-2}]

On GEWEX data, both the all-sky equations are valid within 0.1 Wm^{-2}; see Fig. 8.

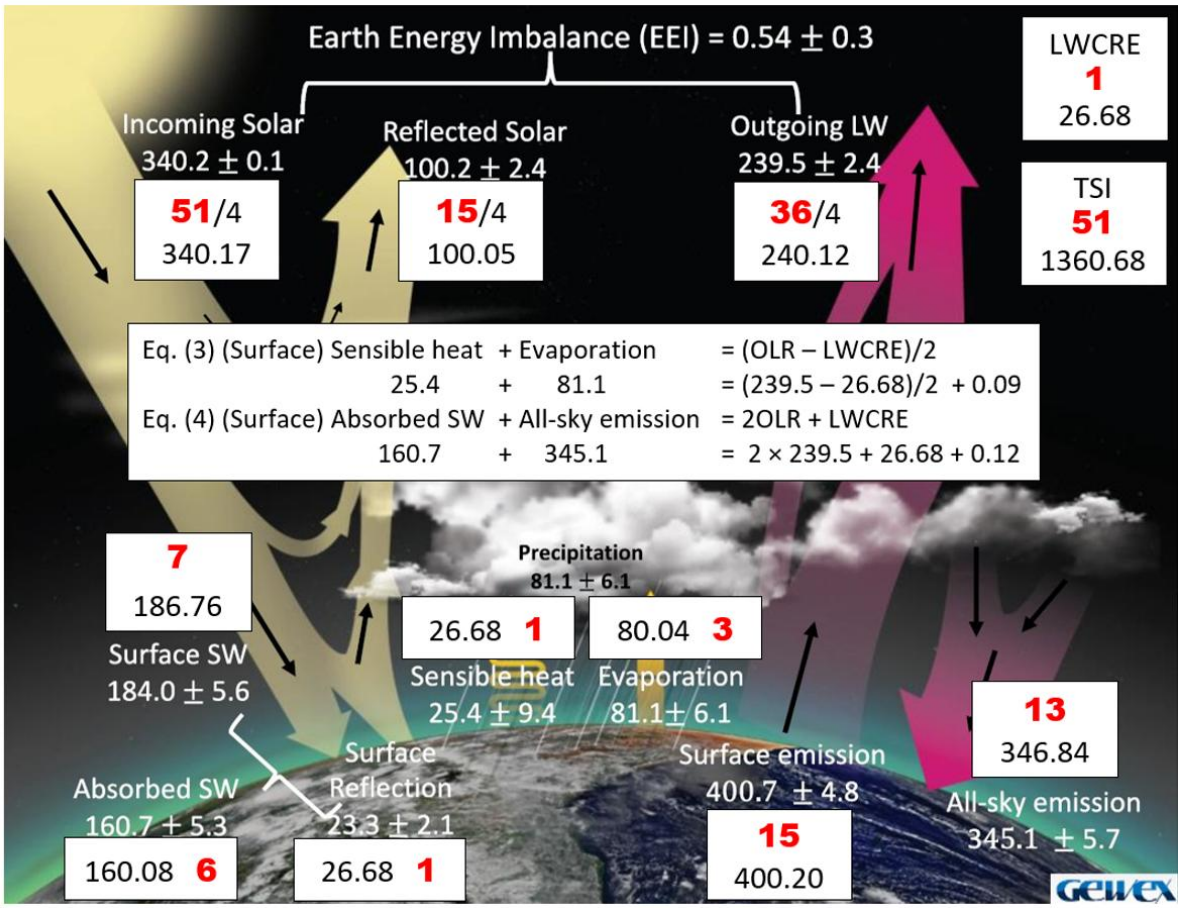

Figure 8 The all-sky (third and fourth) equations and the integer structure is projected on the GEWEX dataset, based on 30 years of data collection (Stephens et al. 2023). The unit flux of LWCRE is a refined value from 26.7 Wm^{-2} from Stephens et al. (2012) to 26.68 Wm^{-2} as the most accurate fit to TSI.

As a comparison, Eq. (3) for convection with the data of Stevens and Schwartz (2012, Table 1), with LWCRE = 26.67 Wm^{-2}: Sensible heat + Latent heat (106) = (OLR – LWCRE)/2 [(239 – 26.67)/2 = 106.165], the difference is 0.165 Wm^{-2}, and Eq. (4) Solar absorbed surface (162) + Back radiation (342) = 2OLR + LWCRE (504.67), the difference is 0.67 Wm^{-2}.

The same with Hartmann's (2016, Fig.2.4) data: Eq. (3) Sensible heat + Latent heat (108) = (OLR – LWCRE)/2 (106.17) is valid with a difference of 1.83 Wm^{-2}, and Eq. (4), Solar absorbed surface (160) Back radiation (345) = 2OLR + LWCRE (504.67) with a difference of 0.33 Wm^{-2}.

Discussion

The integer solution

As the equations are not direct functions of τ, a stationary (geometric) representation may be applied (Fig.9). Let's start with the second equation, stating the equality of the total energy absorbed (and emitted) by the surface to twice the OLR under clear-sky. This case is described by the simplest greenhouse model, see for example Hartmann (1994, Fig. 2.3), representing the flux ratios of $A = 2A_0$ [in Schwarzschild's (1906, Eq. 11) notation] as shown in the upper left panel; Equation (1) is represented in the upper middle panel as $\Delta A = A - E = A_0/2$ and $E = (3/2)A_0$ (for its simple derivation, see Hartmann 1994, Fig. 3.11 and Eq. 3.54).

These three relationships [Eq. (1) as $\Delta A = A - E = A_0/2$, Eq. (2) as $A = 2A_0$, and their immediate corollary, $E = (3/2)A_0$] can be identified on a recently published geometric greenhouse model (Trenberth 2022); for details and its application on the real-Earth atmosphere, see video in the Supplementary Material.

In the right panel of the upper row, the ratios are the same as in the middle, multiplied by 10 (since the unit is not specified yet). Then, introducing the red unit (for LWCRE), and keeping in mind that if Upward LW at TOA is 10 units (of LWCRE) in the clear-sky, then it must by 9 units in the all-sky; and if Downward LW is 12 units in the clear-sky, then it will be 13 units in the all-sky, with the constraint that Upward LW at the surface is the same in both cases, we have an integer ratio system, as shown in Fig.9.

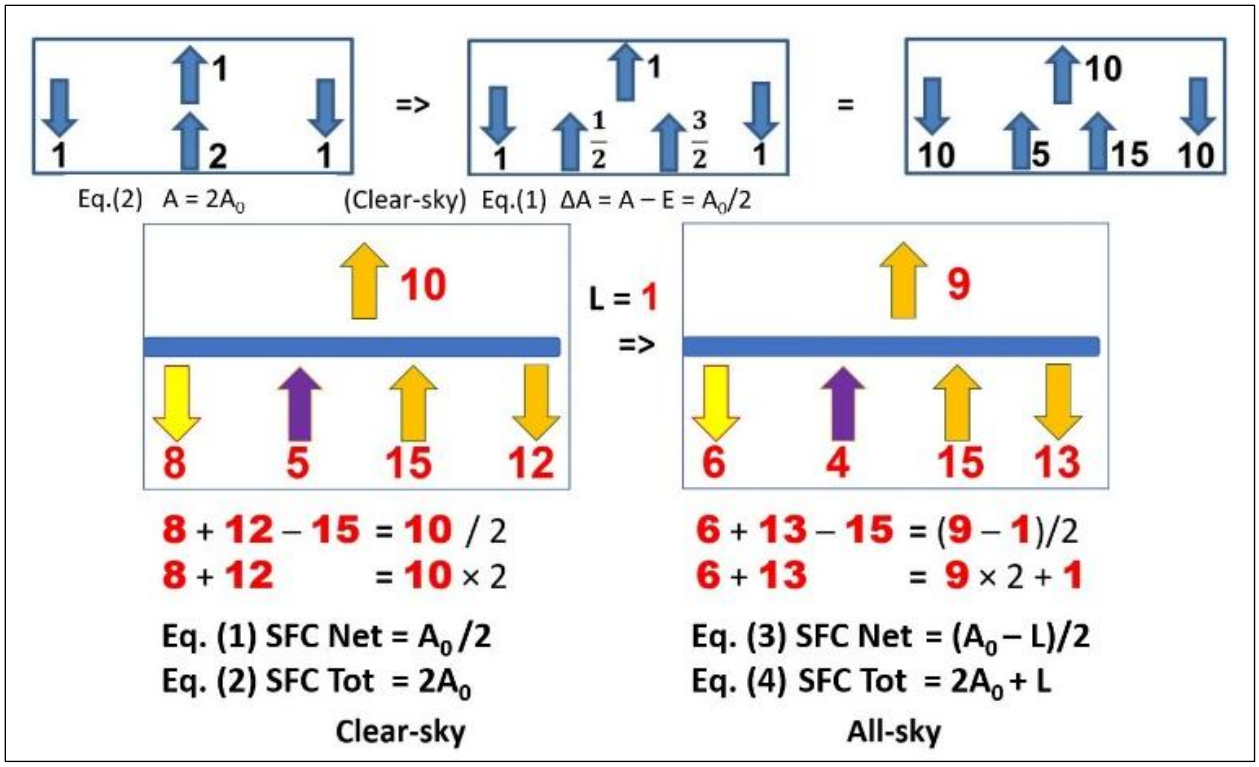

Figure 9 Stationary (geometric) representation of the four equations, with integer solution as multiples of the unit flux of L (representing LWCRE).

Validity of equations and the extended set of the integers on CERES data are given in Table 3. The fit of components not included in the equations (for example, TOA SW up both in clear-sky and all-sky) is remarkable. Notice that the components of convective flux in the GEWEX study (based on the NEWS – NASA Energy and Water-cycle Study methodology, L'Ecuyer et al. 2015) occupy integer positions separately.

Table 3 The four equations and the integer positions for the clear-sky and all-sky global mean energy flow system, including TSI, using the unit flux of 26.68 Wm^{-2} as the best fit on CERES EBAF Ed4.2 data, and the differences. The greenhouse effect is also shown.

Data: CERES EBAF Ed4.2 Version 2, October 2000 – September 2023

Eq. (1) **8** + **12** – **15** = **10**/2; Eq. (2) **8** + **12** = **10** × 2;

Eq. (3) **6** + **13** – **15** = (**9** – **1**)/2; Eq. (4) **6** + **13** = **9** × 2 + **1** **1** = 26.68 Wm^{-2}

TSI = 51 Clear-sky	**N**	**N × Unit (Wm^{-2})**	**EBAF Ed4.2 (Wm^{-2})**	**Diff (Wm^{-2})**
TOA LW up	**40**/4	266.80	265.95	-0.85
TOA SW up	**8**/4	53.36	53.78	0.42
TOA SW net	**3**/4	20.01	20.47	0.46
SFC SW net	**8**	213.44	211.33	-2.11
SFC LW down	**12**	320.16	318.06	-2.10
SFC LW up	**15**	400.20	398.58	-1.62
G	**5**	133.40	132.63	-0.77
TSI = 51 All-sky				
TOA LW up	**36**/4	240.12	240.37	0.25
TOA SW up	**15**/4	100.05	98.95	-1.10
SFC SW net	**6**	160.08	163.71	3.63
SFC LW down	**13**	346.84	346.25	-0.59
SFC LW up	**15**	400.20	398.75	-1.45
G	**6**	160.08	158.38	-1.70

Summary

We recognized small integer ratios between the components of the global mean energy flow system; the fundamental ratios are identified as the solution of four radiative transfer equation having their origin in Schwarzschild's (1906) plane-parallel approximation. Both the ratios and the equations are consistent to global observations of CERES and GEWEX within uncertainty.

As an independent estimate, we recall here the clear-sky greenhouse effect from the GFDL Atmospheric Model 4 (Raghuraman et al. 2019), where its value is referred as 133.4 ± 0.6 Wm^{-2}. Notice that the clear-sky greenhouse factor is g (clear-sky) = G / SFC LW up = 5/15 = 1/3 in the integer system and 132.63/398.58 = 0.333 with CERES data. The integer position for the all-sky greenhouse factor is g(all-sky) = 6/15 = 0.4, while CERES data gives 158.38/398.75 = 0.397.

Using IPCC AR6 data (Forster et al. 2021, Fig. 7.2), the three fundamental climate parameters (Bengtsson 2012) are: Total solar irradiance (51 units in the integer system, 1360.68 Wm^{-2}); planetary albedo (15/51, arithmetically identical to 100/340), and planetary emissivity (TOA LW up / SFC LW up; 9/15 = 0.6 as integer ratio, compared to 239/398 = 0.6005).

References

Ambaum, M. H. P**.** *Thermal Physics of the Atmosphere.* Royal Meteorological Society (2021).

Andrews, D. *An Introduction to Atmospheric Physics*. Cambridge University Press (2010).

Bengtsson, L. Foreword: International Space Science Institute (ISSI) Workshop on Observing and Modeling Earth's Energy Flows. *Surv Geophys* **33**, 333–336 (2012). https://doi.org/10.1007/s10712-012-9194-y

Chamberlain, J. *Theory of Planetary Atmospheres*. Academic Press (1978) (2nd edition: 1987).

Emden, R. (1913) Über Strahlungsgleichgewicht und atmosphärische Strahlung. Sitzungsberichte der mathematisch-physikalischen Klasse der Königlich Bayerischen Akademie der Wissenschaften zu München. English translation: Radiation equilibrium and atmospheric radiation, by H. Bateman. Monthly Weather Review (1916).

Goody, R. *Atmospheric Radiation: Theoretical Basis*. Oxford University Press (1964, 2nd edition with Y.L.Yung, 1989).

Forster, P., T. Storelvmo, K. Armour, W. Collins, J.-L. Dufresne, D. Frame, D.J. Lunt, T. Mauritsen, M.D. Palmer, M. Watanabe, M. Wild, and H. Zhang, 2021: The Earth's Energy Budget, Climate Feedbacks, and Climate Sensitivity. In *Climate Change 2021: The Physical Science Basis. Contribution of Working Group I to the Sixth Assessment Report of the Intergovernmental Panel on Climate Change* [Masson-Delmotte, V., P. Zhai, A. Pirani, S.L. Connors, C. Péan, S. Berger, N. Caud, Y. Chen, L. Goldfarb, M.I. Gomis, M. Huang, K. Leitzell, E. Lonnoy, J.B.R. Matthews, T.K. Maycock, T. Waterfield, O. Yelekçi, R. Yu, and B. Zhou (eds.)]. Cambridge University Press, Cambridge, United Kingdom and New York, NY, USA, pp. 923–1054, doi: 10.1017/9781009157896.009.

Hartmann, D. *Global Physical Climatology*. Academic Press. (1994). (2nd edition: 2016).

Houghton, J. *The Physics of Atmospheres*. Cambridge University Press (1977).

Kopp, G. and J. Lean, A new, lower value of total solar irradiance: Evidence and climate significance. *GRL* **38**, L01706 (2011), https://doi.org/10.1029/2010GL045777

Inamdar, A. and Ramanathan, V. (1997), On monitoring the atmospheric greenhouse effect from space. Tellus B, **49**:216-230, https://doi.org/10.1034/j.1600-0889.49.issue2.8.x

L'Ecuyer, T. S., and Coauthors, The Observed State of the Energy Budget in the Early Twenty-First Century, *J. Climate*, **28**, 8319–8346 (2015) https://doi.org/10.1175/JCLI-D-14-00556.1.

Li, X., Q. Li, M. Wild, P. Jones (2024) An intensification of surface Earth's energy imbalance since the late 20th century. *Nature Comm. EE*, 30 Oct 2024.

Loeb, N. (2014), Langley Colloquium Series & Sigma Series Lecture. NASA Langley Research Center, August 5, 2014.

Loeb, N., Lyman, J., Johnson, G. *et al.* Observed changes in top-of-the-atmosphere radiation and upper-ocean heating consistent within uncertainty. *Nature Geosci* **5**, 110–113 (2012). https://doi.org/10.1038/ngeo1375

NASA CERES CERES_EBAF-Surface_Ed2.8 Data Quality Summary (March 27, 2015).

NASA CERES EBAF Ed4.1_V3 and Ed4.2_V4.

Pierrehumbert, R., *Principles of Planetary Climate*. Cambridge University Press (2008).

Raghuraman, S. P., Paynter, D., & Ramaswamy, V. (2019). Quantifying the drivers of the clear sky greenhouse effect, 2000–2016. *Journal of Geophysical Research: Atmospheres*, 124, 11354–11371. https://doi.org/10.1029/2019JD031017,

Salby, M., *Fundamentals of Atmospheric Physics*. Academic Press (1996).

Salby, M., *Physics of the Atmosphere and Climate*. Cambridge University Press (2012).

Schwarzschild, K. (1906) Ueber das Gleichgewicht der Sonnenatmosphäre. Nachrichten von der Königlichen Gesellschaft der Wissenschaften zu Göttingen. Mathematisch-physikalische Klasse, pp. 41-53, Eq. 11. English translation: Menzel, D. H. (ed), *Selected Papers on the Transfer of Radiation* Dover Publ. (1966)

Stackhouse, P. et al. (2024) State of the Climate in 2023; *Bull. Am. Met. Soc.*, August 2024.

Stephens, G. (2003) Colorado State University AT622 Section 6, Eqs. (6.10a)-(6.10b), Example 6.3, Fig. 6.3a. https://reef.atmos.colostate.edu/~odell/AT622/stephens_notes/AT622_section06.pdf

Stephens, G., Li, J., Wild, M. *et al.* An update on Earth's energy balance in light of the latest global observations. *Nature Geosci* **5**, 691–696 (2012). https://doi.org/10.1038/ngeo1580

Stephens, G., and Coauthors, (1994) The First 30 Years of GEWEX. *Bull. Amer. Meteor. Soc.*, **104**, E126–E157, https://doi.org/10.1175/BAMS-D-22-0061.1.

Stevens, B., Schwartz, S. (2012) Observing and Modeling Earth Energy flows. *Surv Geophys* 33:779-816

Wild, M., Folini, D., Schär, C. *et al.* The global energy balance from a surface perspective. *Clim Dyn* **40**, 3107–3134 (2013). https://doi.org/10.1007/s00382-012-1569-8